IEEE Access
Multidisciplinary | Rapid Review | Open Access Journal

Received 6 December 2023, accepted 29 December 2023, date of publication 1 January 2024, date of current version 6 February 2024.

Digital Object Identifier 10.1109/ACCESS.2023.3349032

RESEARCH ARTICLE

Artificial Hummingbird Optimization Algorithm With Hierarchical Deep Learning for Traffic Management in Intelligent Transportation Systems

ABDULRAHMAN ALRUBAN[1], HANAN ABDULLAH MENGASH[2], MAJDY M. ELTAHIR[3], NABIL SHARAF ALMALKI[4], AHMED MAHMUD[5], AND MOHAMMED ASSIRI[6]

[1]Department of Information Technology, College of Computer and Information Sciences, Majmaah University, Al Majma'ah 11952, Saudi Arabia
[2]Department of Information Systems, College of Computer and Information Sciences, Princess Nourah bint Abdulrahman University, P.O. Box 84428, Riyadh 11671, Saudi Arabia
[3]Department of Information Systems, College of Science & Art at Mahayil, King Khalid University, Saudi Arabia
[4]Department of Special Education, College of Education, King Saud University, Riyadh 12372, Saudi Arabia
[5]Research Center, Future University in Egypt, New Cairo 11835, Egypt
[6]Department of Computer Science, College of Sciences and Humanities at Aflaj, Prince Sattam bin Abdulaziz University, Aflaj 16273, Saudi Arabia

Corresponding author: Abdulrahman Alruban (a.alruban@mu.edu.sa)

The authors extend their appreciation to the Deanship of Scientific Research at King Khalid University for funding this work through large group Research Project under grant number (RGP2/ 29 /44). Princess Nourah bint Abdulrahman University Researchers Supporting Project number (PNURSP2024R114), Princess Nourah bint Abdulrahman University, Riyadh, Saudi Arabia. Research Supporting Project number (RSPD2024R521), King Saud University, Riyadh, Saudi Arabia. Research Supporting Project number (RSPD2024R521), King Saud University, Riyadh, Saudi Arabia. This study is supported via funding from Prince Sattam bin Abdulaziz University project number (PSAU/2023/R/1444). This study is partially funded by the Future University in Egypt (FUE).

ABSTRACT Intelligent Transportation Systems (ITS) make use of advanced technologies to optimize interurban and urban traffic, reduce congestion and enhance overall traffic flow. Deep learning (DL) approaches can be widely used for traffic flow monitoring in the ITS. This manuscript introduces the Artificial Hummingbird Optimization Algorithm with Hierarchical Deep Learning for Traffic Management (AHOA-HDLTM) technique in the ITS environment. The purpose of the AHOA-HDLTM technique is to predict traffic flow levels in smart cities, enabling effective traffic management. Primarily, the AHOA-HDLTM model involves data preprocessing and an Improved Salp Swarm Algorithm (ISSA) for feature selection. For the prediction of traffic flow, the Hierarchical Extreme Learning Machine (HELM) model can be used. The HELM extracts complex features and patterns, with an additional Artificial Hummingbird Optimization Algorithm (AHOA)-based hyperparameter selection process to enhance predictive outcomes. The simulation result analysis under different traffic data demonstrates the better performance of the AHOA-HDLTM technique over existing models. The hierarchical structure of the HELM model along with AHOA-based hyperparameter tuning helps to accomplish enhanced prediction performance. The AHOA-HDLTM technique presents a robust solution for traffic management in ITS, showcasing enhanced performance in forecasting traffic patterns and congestion. The AHOA-HDLTM technique can be used in various smart cities and urban regions. Its abilities in real-time traffic flow prediction can be helpful in the design of efficient, sustainable, and resilient transportation networks.

INDEX TERMS Smart cities, intelligent transportation system, deep learning, traffic management, feature selection.

I. INTRODUCTION

In urban areas, high population growth leads to a growth in carbon emissions, air pollution, and traffic congestion which impact the environment negatively but also delay economic growth and the life quality of people [1]. To overcome this

The associate editor coordinating the review of this manuscript and approving it for publication was Shaohua Wan.

challenge, intelligent transportation systems (ITS) have been developed for the solution. Integrating advanced methodologies like the Internet of Things (IoT), artificial intelligence (AI), and machine learning (ML) can improve transportation security, sustainability, and efficiency [2]. ITS is the main part of smart cities that can aid in improving the employment of transportation infrastructure, enhance mobility for citizens, and decrease traffic congestion. Traffic forecasts offer experts a period to propose resource provisions to safeguard a safe journey [3]. By congestion, the worth of street networks is restricted. The decreases outcome in direct as well as indirect charges for the public. The congestion effects on the social structure and economic system have been researched widely [4]. Prediction of traffic flow is regarded as one of the time-series-based issues because the future cost of traffic flow has been assessed based on the previous data from one or more locations. The volume of data develops the big data idea in the transportation field from a wide range of sources. Depending upon the sort of data gathered, dissimilar artificial intelligence (AI) techniques are utilized to value the overload parameters [5]. There are many methods for analyzing and storing so big data have a risky effect on the prediction task. The development of big data computing amenities provides chances for attaining exactness in traffic data prediction [6].

In recent times, AI and MI field has stemmed from the capability to expect traffic congestion. Recently, this study area has extended owing to the arrival of enormous information from static sensor networks [7]. Numerous traffic factors have been estimated to anticipate traffic congestion, especially short-term congestion issues. Most researchers on expecting traffic congestion use previous data. Whereas, a few researchers have expected congestion issues in the real period [8]. Congestion forecasting is one of the most challenging issues to resolve from the view of modifiability when compared to traffic flow forecast in non-congested situations. However, the Traffic supervisors implemented relief actions to the alarm system. The shallow design technique has been utilized for the prediction task in most cases. This framework offers effective solutions for the small size of data only but does not support big traffic data [9]. In recent days, a Deep learning (DL) framework such as deep belief network (DBN), DNN, recurrent neural networks (RNN), and CNN utilized in several difficult applications such as video analysis, large data set for image, natural language procedure and also in several data mining procedure [10].

This manuscript presents an Artificial Hummingbird Optimization Algorithm with Hierarchical Deep Learning for Traffic Management (AHOA-HDLTM) technique in the ITS environment. The AHOA-HDLTM technique initially performs data preprocessing and improved salp swarm algorithm (ISSA) based feature selection. For traffic flow monitoring, the AHOA-HDLTM method applies a hierarchical ELM (HELM) model. At last, the predictive result of the HELM approach can be upgraded by the use of an AHOA-based hyperparameter selection process. The enhanced performance of the AHOA-HDLTM method can be assured using a detailed simulation analysis of diverse traffic data.

II. LITERATURE REVIEW

Abdullah et al. [11] designed a bi-directional RNN (BRNN) employing GRU. The method employs a BRNN to fake and predict traffic congestion in the smart areas. This study recommends a data-driven model by utilizing BRNN for traffic organization that employs real-time information from devices and connected mechanisms to control traffic efficiently. In [12], an enhanced solution is designed, which integrates a novel target tracing and moving vehicle counting technique and a better LSTM system for the forecast of traffic flow. Specifically, the MultiNetV3 framework and DCN V2 convolution kernel are mainly employed to exchange YOLOv4's traditional convolutional kernel and backbone network to recognize multiple targets tracking and moving separately.

In [13], an effectual approach for OD (Origin–Destination) matrix forecast depends on traffic info employing DL. The model using DNN with the LSTM or autoencoder layers is categorized by comparatively high resistance and accuracy to miss data from temporary measurement points that are located in the urban road network. In [14], a new DL design called Ensemble Attention-based Graph Time Convolutional Networks (EAGTCN) is designed. At the initial stage, by spatial blocks, the global spatial pattern is captured which are attached by a three-dimensional ensemble attention layer as well as a Graph Convolution Network (GCN). In [15], a temporal threshold mechanism and soft spatial is designed. To fill out the absent weather info spatial interpolation methods were utilized. Hybrid DL techniques such as CNN-LSTM and LSTM are also proposed. The hybrid method eliminates the features of spatiotemporal and later employs these features as memory. This method forecasts the traffic stream variances based on past features as well as time-based input. Qi et al. [16] presented a DL model depending on a spatiotemporal GCN. This model consists of four processes. First, creating a biased adjacency matrix utilizing the Gaussian similarity function. Second, accumulating a feature matrix. Lastly creating a spatiotemporal GCN depend on a DL design (i.e. T-GCN).

Yang et al. [17] present a traffic flow dependency and dynamics-based DL-aided method (TD2-DL). Exactly, the graph theory-based model is proposed to classify the local temporal-spatial traffic dependency. Next, the LSTM model is used. Last, an EKF is applied for integrating the expected traffic speed that is projected by v-CTM joined with the LSTM and the field traffic information. So, the FNN technique has been mainly developed. In [18], a PSO-BiLSTM method depends on the integration of BiLSTM neural network and PSO is proposed. The PSO model searches for the optimal parameters on a total scale that has been utilized and then non-linear adjustable inertial weights are taken rather than linear weights. In addition to that, the BiLSTM prediction technique of the network is enhanced by employing the PSO method.

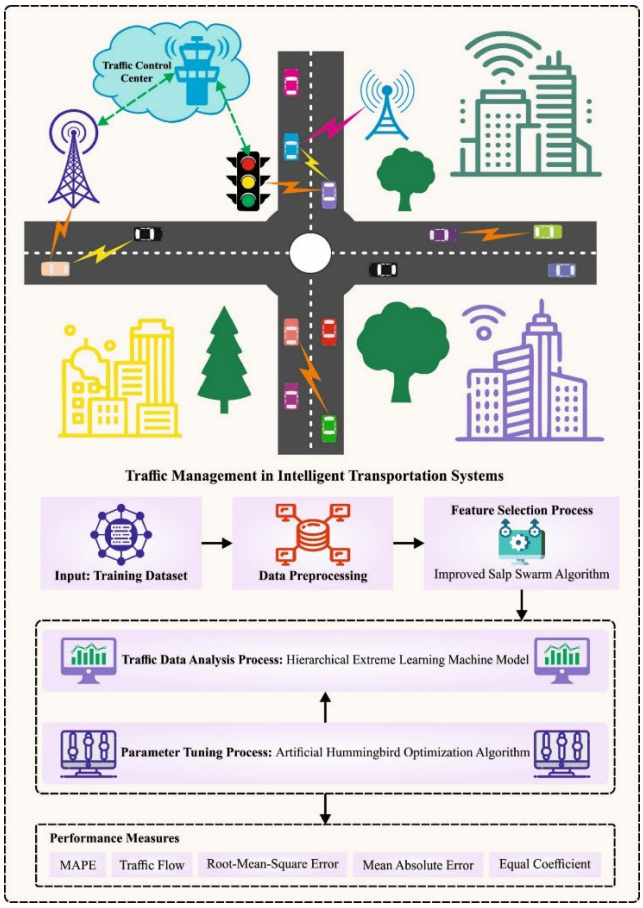

FIGURE 1. Workflow of AHOA-HDLTM algorithm.

In [19], a traffic flow recognition technique that depends on DL on the edge node has been presented. Initially, the authors present a vehicle recognition technique that depends on the YOLOv3 method trained with a great volume of traffic data. Yu et al. [20] present a DL-based traffic safety performance for a mixture of autonomous and manual vehicles from a 5G-enabled ITS. In [21], cloud-assisted IoT-ITS (CIoT-ITS) was presented to overcome traffic management problem. At this point, the IoT sensor combined camera has been installed in the entire traffic signal corner for monitoring the vehicle's flow. Chen et al. [22] examine energy-efficient and regenerative energy recovery systems for sustainable ITS utilizing Artificial societies, Computational experiments, and Parallel execution (ACP) structure.

III. THE PROPOSED MODEL

In this manuscript, a novel AHOA-HDLTM method is established in the ITS environment. The main purpose of the AHOA-HDLTM system is to predict the level of traffic flow in the ITS, enabling proper traffic management in smart cities. To accomplish this, the AHOA-HDLTM technique encompasses data preprocessing, ISSA-based FS, HELM-based classification, and AHOA-based parameter tuning. Fig. 1 shows the workflow of the AHOA-HDLTM technique.

A. DATA PREPROCESSING

Min-max normalized called feature scaling, is a generally employed method in traffic flow monitoring and data preprocessing. It changes and scales the range of numerical data to a certain range, usually between zero and one, making it appropriate for many ML and data analysis tasks. In the context of traffic flow monitoring, min-max normalized can be executed for numerical features like traffic speed, volume, or occupancy.

B. FEATURE SELECTION USING ISSA

The ISSA is used for electing an optimum subset of features. SSA is a recent bio-inspired technique based on the foraging and navigation of salp in the ocean [23]. A leader and followers are the two groups performed in SSA. The solution candidate is based on the salp location while foraging and navigation, usually for optimization problems is treated as a 2D matrix known as x. The present optimum solution is known as a food source, F_j, and the leader location of salp, x_j^1 is updated according to Eq. (1):

$$x_j^1 = \begin{cases} F_j + c_1\left(\left(ub_j - lb_j\right)c_2 + lb_j\right), & c_3 \geq r \\ F_j + c_1\left(\left(ub_j - lb_j\right)c_2 + lb_j\right), & c_3 < r \end{cases} \tag{1}$$

where the up and low boundaries of the searching space are ub_{j} *and* lb_{j}, the uniformly distributed random integer within [0, 1] are r,c_2 and c_3 parameters that are embedded in the SSA. The c_1 parameter is then evaluated by Eq. (2):

$$c_1 = 2e^{-(4t/T)^2} \tag{2}$$

where the existing and the maximal iterations that should be initially set are t and T. The follower location of salps is evaluated by Eq. (3):

$$x_j^i = \frac{1}{2}\left(x_j^i + x_j^{i-1}\right) i \geq 2 \tag{3}$$

The salp follower will be completely directed by the leader in the original SSA to discover the optimum solution according to the region of possible solution is evaluated through the change among the upper and lower limitations of the control variable. Once the problem dimension is considered smaller, then it performs well. Nonetheless, if the search for a possible solution is large, then the exploitation process becomes ineffective. In resolving the optimization problem, the balance between exploitation and exploration needs to be decided wisely, note that the exploration capability of SSA is quite restricted. In this work, two enhancements will be suggested for enhancing the exploitation-exploration abilities. The improved version is performed in Eq. (1), but the low boundary has been removed to enhance the process's capability to use resources that are formulated by Eq. (4):

$$x_j^1 = \begin{cases} F_j + c_1\left(\left(ub_j - lb_j\right)c_2\right), & c_3 \geq r \\ F_j + c_1\left(\left(ub_j - lb_j\right)c_2\right), & c_3 < r \end{cases} \tag{4}$$

The second enhancement is executed to enhance the exploration ability, where follower expression in Eq. (3) is

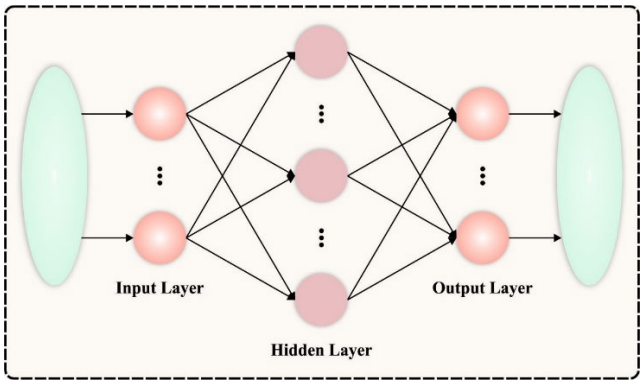

FIGURE 2. ELM structure.

transformed into:

$$x_j^i = \left(px_j^i + qx_j^{i-1}\right) i \geq 2 \tag{5}$$

In Eq. (5), p is a random integer [0, 1] and q is evaluated as $(1 - p)$.

The fitness function (FF) employed in the ISSA methodology has been presented to take a balance amongst the count of preferred features from the entire outcome (lesser) and classification outcome (higher) acquired through applying chosen feature, Eq. (6) refers to the FF for measuring outcomes.

$$Fitness = \alpha\gamma_R(D) + \beta\frac{|R|}{|C|} \tag{6}$$

In Eq. (6), $\gamma_R(D)$ stands for the classifier error rate of the offered classifier. $|R|$ implies the cardinality of the chosen subset and $|C|$ denotes complete feature counts in the database, parameters α and β are equivalent to the impact of classification algorithm quality and subset length.

C. HELM BASED PREDICTION

To forecast the traffic flow, the HELM approach is utilized. ELM is initially presented to train SLFNs [24]. A prominent feature of ELM is that the parameters among the hidden and input layers (HL) can be arbitrarily created and the only free parameters, which require that optimizer are the resultant weights among the HL and the resultant state. Fig. 2 illustrates the infrastructure of ELM. To provide a training set $\left\{(x_i, t_i) \mid x_i \in \mathbb{R}^d, t_i \in \mathbb{R}, i = 1, \ldots, N\right\}$, whereas x_i implies the trained data and t_i denotes the target. SLFNs network function with L hidden node (HN) is defined as:

$$f_L(x) = \sum_{j=1}^{L} G_j(x) * \beta_j, \beta_j \in \mathbb{R} \tag{7}$$

In which, β_j implies the weighted linking of the j^{th} HN to the output node and G_j represents the j^{th} HN resultant function. To additive nodes with activation function g, G_j is expressed as:

$$G_j(x) = g\left(a_j \cdot x + b_j\right), \quad a_j \in \mathbb{R}^d, \mathrm{b_j} \in \mathbb{R} \tag{8}$$

whereas a_j refers to the weighted vector linking the input layer to j^{th} HN and b_j is the biases of j^{th} HN, To the RBF node with initiation function g, G_j is represented as:

$$G_j(x) = g\left(\frac{\|x - a_j\|}{b_j}\right), \mathrm{a_j} \in \mathbb{R}^d, b_j \in \mathbb{R}^+ \tag{9}$$

whereas a_j and b_j denote the centre and effect factor of the j^{th} RBF node.

To trained data $X = [x_1, x_2, \ldots, x_N]^T \in \mathbb{R}^{N \times d}$ that contains N instances with all the samples are a d-dimensional vector, $T = (t_1, t_2, \ldots t_N)^T \in \mathbb{R}^{N \times 1}$ refers to the equivalent target matrix. Simple ELM purposes for obtaining the resultant weight by decreasing the amount of predictive error and the norm of resultant weights:

$$\min \|H\beta - T\|^2 + \lambda\|\beta\|^2 \tag{10}$$

whereas $H = [h_1, h_2, \ldots, h_N]^T \in \mathbb{R}^{N \times L}$ inferred the arbitrary latent representation matrix of the input X. It can be attained by Eq. (8) or (9) with a_j parameter , b_j arbitrarily created and $h_i = (G_1(x_i), G_2(x_i), \ldots G_L(x_i))^T$, $i = 1, 2, \ldots N$. λ implies regularized hyperparameter.

$$\beta^* = (H^T H + \lambda I)^{-1} H^T T \tag{11}$$

Once the hidden neuron counts L is lesser than the count of trained data N. When the hidden neuron counts are superior to the amount of trained data, a better performance is:

$$\beta^* = H^T (HH^T + \lambda I)^{-1} T \tag{12}$$

H-ELM is acquired in 2 phases. Primarily, similar to typical DL approaches, K unsupervised ELM-SAEs are fixed for learning K layers of latent representation *Rnd* the learned representation (R) of the preceding element has been utilized as input of the next element.

$$R_i = s(R_{i-1}\left(\beta_i^*\right)^T) \tag{13}$$

In which, R_i denotes the learned representation of i^{th} HL (the significant representation extracted by i^{th} ELM sparse AE), R_{i-1} implies the learned representation of $i - l$ th HL and it is additionally utilized as the input of $i-1$ component. β_i^* denotes the better-recreated matrix of i^{th} ELM sparse AE that obtains R_{i-1} as input, and s denotes the activation function of HLs. When the feature in the preceding HL has been extracted, the weighted matrix of existing HL is set and requires not to be adjusted.

D. AHOA-BASED PARAMETER TUNING

Finally, the AHOA approach can be executed for the parameter tuning process. AHOA performs the optimizer by the natural behavior of hummingbirds [25]. It primarily contains 3 components namely visit table, food sources, and population (No. of hummingbirds). While handling the foraging state, it again consists of three diverse approaches migrating foraging, guided foraging, and territorial foraging. The mathematical formula can be discussed in the following.

Step1: Initialization: Let h be a number of birds and prey for the optimizer. It can be established randomly.

$$f_j = LB + n \cdot (UB - LB), j = 1, 2, \ldots, h \tag{14}$$

where n is the random number range from zero to one. Here, the visit table can be described as the visit level of food sources for respective birds. The visit level proves more important. Hereafter, each bird attacks the food via the visit table.

The food source is initialized in the visit table shown below:

$$st_{i,k} = \begin{cases} 0 \ \ if \ j \neq k \\ null \ j = k \end{cases}, \quad \mathrm{j},k = 1, 2, \ldots, h \tag{15}$$

Now, *null* represents the food captured by hummingbirds, the 0 value signifies that k^{th} food is visited by j^{th} bird.

Step2: Guided searching:- This behavior can be stimulated by the visit stage of the food source. When the food is targeted, the hummingbird flies to feed it. The flying or flight nature relies on 3 directions namely axial, omnidirectional, and diagonal flights.

$$G_{af}^{j} = \begin{cases} 1 & \text{if } j = rdj\left([1,z]\right), j = 1, \ldots, z \\ 0 & otherwise \end{cases} \tag{16}$$

$$G_{df}^{j} = \begin{cases} if \ = D(k), \in [1,], \\ 1D = rdp(), \\ i \in [2, \ (n_1 \cdot (z-2)) + 1] \\ 0 \ otherwise \end{cases} \quad j = 1, \ldots, z \tag{17}$$

$$G_{of}^{j} = 1 \quad j = 1, \ldots, z \tag{18}$$

where $rdj([1,z])$ and $p(i)$ respectively are the randomly generated integer and permutation integer. Furthermore, the random value is taken from 0 to 1 using the parameter n_1. A candidate food source can be obtained by these flights.

The prey can be modernized from old to another location.

$$g_j\left(b+1\right) = f_{j,tg}\left(b\right) + \alpha \cdot G \cdot \left(f_j\left(b\right) - f_{j,tg}\left(b\right)\right) \tag{19}$$

In Eq. (19), the prey position and targeted prey are stated as $f_i\left(b\right)$ and $f_{i,tg}(b)$, correspondingly. Next, the guided feature as $\alpha \sim R(0, 1)$ shows the uniform distribution function with mean 0 and standard deviation (SD) 1.

$$f_j\left(b+1\right) = \begin{cases} f_j\left(b\right) & FT\left(f_j\left(b\right)\right) \leq FT\left(g_j\left(b+1\right)\right) \\ g_j\left(b+1\right) & FT\left(f_j\left(b\right)\right) > FT\left(g_j\left(b+1\right)\right) \end{cases} \tag{20}$$

Step3: Territorial searching: -When the target prey has been visited that can consumed already, afterwards it can visit novel or other food sources in their territory. The new location is produced by means of Eq. (21) based on the respective area.

$$g_j\left(b+1\right) = f_j\left(b\right) + \beta \cdot G \cdot f_j\left(b\right) \tag{21}$$

where β shows the territorial factor as $\sim R\left(0, 1\right)$.

Step4: Migration searching: The repeated visiting lacks the food source in the territorial area. A migration co-efficient has been considered the worst nectar-refilling rate. It transfers towards a novel target. Therefore, it assumes random generation of food sources by worse nectar.

$$f_{wrst} = LB + n.\left(UB - LB\right) \tag{22}$$

As a result, the optimum solution is attained from AHOA which is used for parameter selection.

During this case, the AHOA has been deployed for determining the hyperparameter contained in the HELM algorithm. The MSE has assumed that the main purpose is written as:

$$MSE = \frac{1}{T}\sum_{j=1}^{L}\sum_{i=1}^{M}\left(y_j^i - d_j^i\right)^2 \tag{23}$$

whereas M and L denote the outcome value of state and data, y_j^i and d_j^i denote the gained and suitable magnitudes for $thej^{th}$ unit from the outcome state of the network in time t correspondingly.

IV. PERFORMANCE VALIDATION

The AHOA-HDLTM approach has been validated utilizing the traffic data comprising every 30s raw sensor information for 30 days. The traffic information gathered in the 1st 10 days has been utilized as a training database the database comprising the data for the remaining 20 days can be employed as a testing database. During this research, the group of data comprised of 15min of combined data in vehicles per 15 minutes (veh per 15 minutes). Therefore, 96 data groups can be accessible every day. Earlier in the computation, the group of data was normalised and the information was rendered from the range of zero to one.

Table 1 and Fig. 3 provide the overall predictive outcomes of the AHOA-HDLTM technique in terms of MAPE. The outcomes imply that the AHOA-HDLTM technique exhibits effectual traffic flow prediction results under several iterations. It is also noticed that the MAPE values are decreased with a rise in iterations. It is identified that the AHOA-HDLTM technique attains the best fitness of 0.23 average fitness of 0.94 and worst fitness of 2.61 under iteration 100.

TABLE 1. MAPE outcome of AHOA-HDLTM system at distinct iterations.

MAPE (%)			
No. of Iterations	Best Fitness	Average Fitness	Worst Fitness
0	1.50	4.98	7.47
10	0.68	2.69	7.02
20	0.29	0.84	4.52
30	0.47	0.90	4.21
40	0.53	1.30	4.52
50	0.34	1.06	3.89
60	0.42	0.56	3.38
70	0.32	1.20	3.17
80	0.39	0.99	2.66
90	0.24	0.27	2.77
100	0.23	0.94	2.61

Table 2 and Fig. 4 represent the actual vs. predicted traffic flow of the AHOA-HDLTM technique under vary-

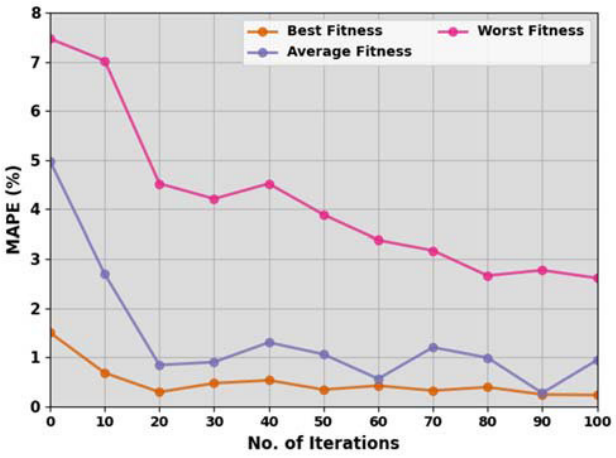

FIGURE 3. MAPE outcome of AHOA-HDLTM system under various iterations.

TABLE 2. Traffic flow outcome of AHOA-HDLTM algorithm under various runs.

Traffic Flow						
Time Index	Actual	Predicted				
		Run_1	Run_2	Run_3	Run_4	Run_5
0	193	229	233	247	236	268
10	139	132	132	119	93	90
20	887	899	863	867	924	919
30	967	968	978	984	930	938
40	726	699	661	656	655	623
50	774	803	838	799	805	791
60	960	975	995	1010	989	953
70	863	872	833	836	882	893
80	970	1024	1039	1031	1014	1053
90	1041	1042	1042	1021	965	955
100	615	639	604	614	564	547

ing runs and time indexes. The obtained values pointed out that the AHOA-HDLTM technique effectually predicted the flow of traffic under all runs. It is also noticed that the AHOA-HDLTM technique accomplishes effectual outcomes under all time indices.

Table 3 illustrates the comparative outcome of the AHOA-HDLTM technique with recent techniques with respect to Root Mean Square Error (RMSE), Mean Absolute Error (MAE), and equal coefficient (EC) [26].

Fig. 5 represents the RMSE inspection of the AHOA-HDLTM technique with recent approaches. The outcomes indicate that the PSOLS-SVM and FFOLS-SVM systems are depicted as ineffective performance with maximal RMSE values. Besides, the hybrid LSSVM model has attained a somewhat lesser RMSE value whereas the AST2-FPOHDBN and IAROEL-TFMS algorithms have attained considerable RMSE values. However, the AHOA-HDLTM system reports effectual outcomes with minimal RMSE values of 20.226, 17.306, 15.684, 22.261, and 17.321 under lags 1-5, correspondingly.

Fig. 6 demonstrates the MAE outcome of the AHOA-HDLTM method with recent approaches. The outcomes signify that the PSOLS-SVM and FFOLS-SVM models have

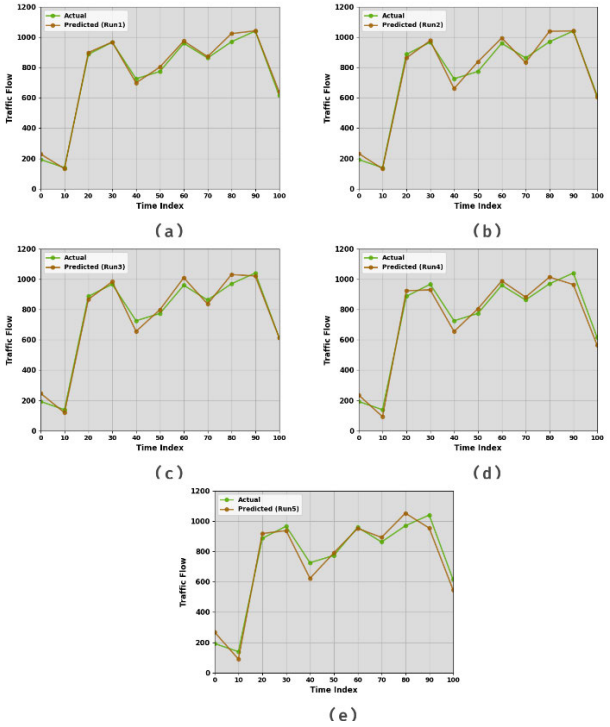

FIGURE 4. Traffic flow outcome of AHOA-HDLTM algorithm (a-e) Runs 1-5.

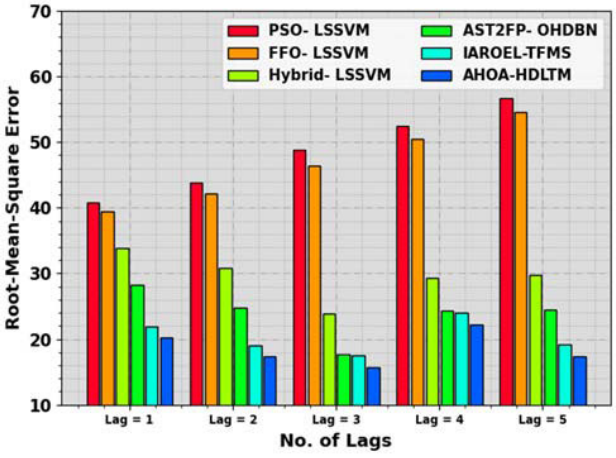

FIGURE 5. RMSE outcome of AHOA-HDLTM system under all lags.

shown ineffective performance with maximal MAE values. Also, the hybrid LSSVM algorithm has attained a somewhat decreased MAE value whereas the AST2-FPOHDBN and IAROEL-TFMS systems have gained considerable MAE values. But, the AHOA-HDLTM technique reports effective outcomes with lesser MAE values of 13.777, 11.186, 15.693, 20.880, and 17.531 under lags 1-5, correspondingly.

In Fig. 7, the EC results of the AHOA-HDLTM technique are compared with recent models. The outcome highlighted that the AHOA-HDLTM technique offers improved performance with increased EC values under all lags. On lag 1, the AHOA-HDLTM technique provides a higher EC of 99.42 whereas the PSOLS-SVM, FFOLS-SVM, Hybrid

TABLE 3. Comparative outcome of AHOA-HDLTM system with recent models under all lags.

No. of Lags	PSOLS-SVM	FFOLS-SVM	Hybrid LS-SVM	AST2FP OH-DBN	IAROEL-TFMS	AHOA-HDLTM
Root-Mean-Square Error						
Lag = 1	40.748	39.520	33.883	28.316	21.916	20.226
Lag = 2	43.887	42.146	30.851	24.706	19.016	17.306
Lag = 3	48.880	46.371	23.872	17.614	17.574	15.684
Lag = 4	52.487	50.548	29.311	24.281	24.001	22.261
Lag = 5	56.702	54.532	29.798	24.531	19.141	17.321
Mean Absolute Error						
Lag = 1	26.101	23.401	23.213	16.907	15.517	13.777
Lag = 2	33.292	26.541	20.410	13.586	13.056	11.186
Lag = 3	40.864	32.838	24.849	19.323	17.413	15.693
Lag = 4	48.276	38.580	28.514	21.660	22.700	20.880
Lag = 5	53.663	46.022	25.905	21.191	19.331	17.531
Equal Coefficient						
Lag = 1	95.85	95.96	98.08	98.51	99.24	99.42
Lag = 2	95.71	95.92	98.03	98.67	99.13	99.28
Lag = 3	95.48	95.58	98.71	98.95	99.21	99.37
Lag = 4	95.28	95.41	98.56	98.78	99.32	99.59
Lag = 5	95.05	95.25	97.40	98.78	99.47	99.71

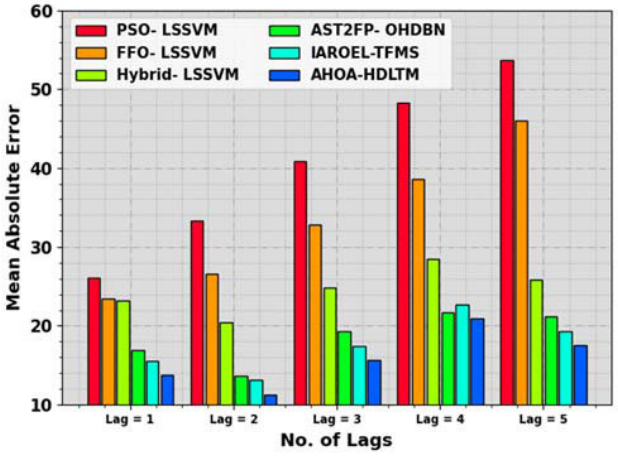

FIGURE 6. MAE outcome of AHOA-HDLTM methodology under all lags.

LS-SVM, AST2-FPOHDBN, and IAROEL-TFMS models accomplish lower EC of 95.85%, 95.96%, 98.08%, 98.51%, and 99.24%, respectively. Additionally, on lag 5, the AHOA-HDLTM method offers superior EC of 99.71 whereas the PSO- LSSVM, FFOLS-SVM, Hybrid LS-SVM, AST2-FPOHDBN, and IAROEL-TFMS systems gain lesser EC of 95.05%, 95.25%, 97.40%, 98.78%, and 99.47%, correspondingly.

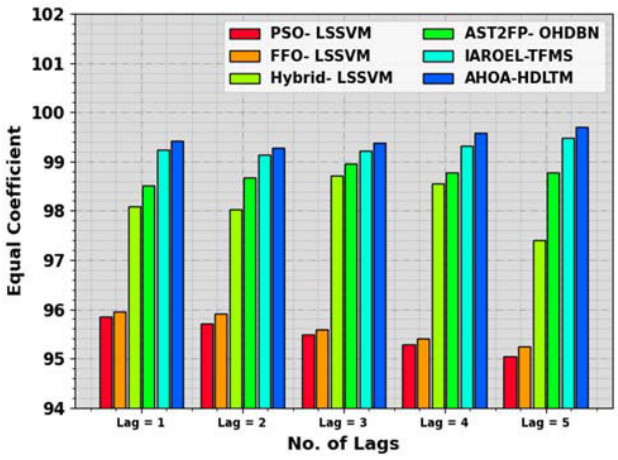

FIGURE 7. EC outcome of AHOA-HDLTM approach under all lags.

TABLE 4. RUNT outcome of AHOA-HDLTM approach with recent models under all lags.

Running Time (sec)						
No. of Lags	PSOLS-SVM	FFOLS-SVM	Hybrid LS-SVM	AST2FP OH-DBN	IAROEL-TFMS	AHOA-HDLTM
Lag = 1	11.45	14.38	9.98	3.99	2.26	1.06
Lag = 2	11.78	14.61	10.16	3.75	2.75	1.18
Lag = 3	11.79	15.21	10.19	5.27	4.22	2.61
Lag = 4	12.29	15.41	10.20	5.21	3.81	2.14
Lag = 5	12.36	15.43	10.62	5.20	4.42	3.06

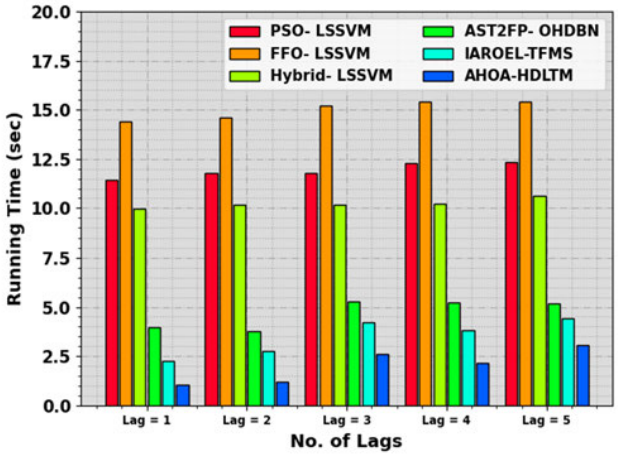

FIGURE 8. RUNT outcome of AHOA-HDLTM approach under all lags.

Table 4 and Fig. 8 represent the running time (RUNT) inspection of the AHOA-HDLTM technique with recent models. The results indicate that the PSOLS-SVM and FFOLS-SVM models have shown ineffective performance with maximum RUNT values. At the same time, the hybrid LSSVM model has attained a slightly decreased RUNT value whereas the AST2-FPOHDBN and IAROEL-TFMS models have obtained considerable RUNT values. Nevertheless, the

AHOA-HDLTM technique reports effectual outcomes with minimal RUNT values of 1.06s, 1.18s, 2.61s, 2.14s, and 3.06s under lags 1-5, correspondingly. These results confirmed the enhanced predictive results of the AHOA-HDLTM method.

V. CONCLUSION

In this manuscript, a new AHOA-HDLTM method was developed in the ITS environment. The main purpose of the AHOA-HDLTM system is to forecast the level of traffic flow in the ITS, enabling proper traffic management in smart cities. To accomplish this, the AHOA-HDLTM approach includes data preprocessing, ISSA-based feature selection, HELM-based classification, and AHOA-based parameter tuning. For traffic flow monitoring, the AHOA-HDLTM technique uses the HELM model, tailored for traffic data analysis, and extracts intricate features and patterns. At last, the predictive outcome of the HELM technique can be better by using an AHOA-based hyperparameter selection process. The enhanced performance of the AHOA-HDLTM method can be assured using a detailed simulation analysis of diverse traffic data. The extensive results highlighted the better predictive outcome of the AHOA-HDLTM system with other methods. While the article primarily focuses on traffic flow prediction through the AHOA-HDLTM approach, there exists a critical avenue for further investigation into the intricate interconnection between traffic flow and traffic state.

ACKNOWLEDGMENT

The authors extend their appreciation to the Deanship of Scientific Research at King Khalid University for funding this work through large group Research Project under grant number (RGP2/ 29 /44). Princess Nourah bint Abdulrahman University Researchers Supporting Project number (PNURSP2024R114), Princess Nourah bint Abdulrahman University, Riyadh, Saudi Arabia. Research Supporting Project number (RSPD2024R521), King Saud University, Riyadh, Saudi Arabia. Research Supporting Project number (RSPD2024R521), King Saud University, Riyadh, Saudi Arabia. This study is supported via funding from Prince Sattam bin Abdulaziz University project number (PSAU/2023/R/1444). This study is partially funded by the Future University in Egypt (FUE).

REFERENCES

[1] L. Jiang, T. G. Molnár, and G. Orosz, "On the deployment of V2X roadside units for traffic prediction," *Transp. Res. C, Emerg. Technol.*, vol. 129, Aug. 2021, Art. no. 103238.

[2] X. Shi, H. Liu, M. Wang, X. Li, B. Ciuffo, D. Work, and D. Kan, "Inconsistency of AV impacts on traffic flow: Predictions in literature," in *Proc. Automated Road Transp. Symp.* Cham, Switzerland: Springer, Jul. 2022, pp. 165–173.

[3] A. Okic, L. Zanzi, V. Sciancalepore, A. Redondi, and X. Costa-Pérez, "P-ROAD: A learn-as-you-go framework for on-demand emergency slices in V2X scenarios," in *Proc. IEEE Conf. Comput. Commun. (INFOCOM)*, May 2021, pp. 1–10.

[4] W. Qi, B. Landfeldt, Q. Song, L. Guo, and A. Jamalipour, "Traffic differentiated clustering routing in DSRC and C-V2X hybrid vehicular networks," *IEEE Trans. Veh. Technol.*, vol. 69, no. 7, pp. 7723–7734, Jul. 2020.

[5] C. Backfrieder, G. Ostermayer, and C. F. Mecklenbräuker, "Increased traffic flow through node-based bottleneck prediction and V2X communication," *IEEE Trans. Intell. Transp. Syst.*, vol. 18, no. 2, pp. 349–363, Jul. 2016.

[6] R. Song, L. Lyu, W. Jiang, A. Festag, and A. Knoll, "V2X-boosted federated learning for cooperative intelligent transportation systems with contextual client selection," 2023, *arXiv:2305.11654*.

[7] L. Luo, L. Sheng, H. Yu, and G. Sun, "Intersection-based V2X routing via reinforcement learning in vehicular ad hoc networks," *IEEE Trans. Intell. Transp. Syst.*, vol. 23, no. 6, pp. 5446–5459, Feb. 2021.

[8] T. Xu, J. Guan, Y. Hao, and D. Sun, "Real-time traffic state predictor based on dynamic traveller behaviour," *Proc. Inst. Civil Eng.-Transp.*, vol. 176, no. 5, pp. 290–300, Aug. 2023.

[9] X. Yuan, J. Chen, J. Yang, N. Zhang, T. Yang, T. Han, and A. Taherkordi, "FedSTN: Graph representation driven federated learning for edge computing enabled urban traffic flow prediction," *IEEE Trans. Intell. Transp. Syst.*, pp. 1–11, 2022.

[10] E. Zadobrischi, L.-M. Cosovanu, and M. Dimian, "Traffic flow density model and dynamic traffic congestion model simulation based on practice case with vehicle network and system traffic intelligent communication," *Symmetry*, vol. 12, no. 7, p. 1172, Jul. 2020.

[11] S. M. Abdullah, M. Periyasamy, N. A. Kamaludeen, S. K. Towfek, R. Marappan, S. K. Raju, A. H. Alharbi, and D. S. Khafaga, "Optimizing traffic flow in smart cities: Soft GRU-based recurrent neural networks for enhanced congestion prediction using deep learning," *Sustainability*, vol. 15, no. 7, p. 5949, Mar. 2023.

[12] Y. Zheng, X. Li, L. Xu, and N. Wen, "A deep learning–based approach for moving vehicle counting and short-term traffic prediction from video images," *Frontiers Environ. Sci.*, vol. 10, May 2022, Art. no. 905443.

[13] T. Pamuła and R. Żochowska, "Estimation and prediction of the OD matrix in uncongested urban road network based on traffic flows using deep learning," *Eng. Appl. Artif. Intell.*, vol. 117, Jan. 2023, Art. no. 105550.

[14] B. Yao, A. Ma, R. Feng, X. Shen, M. Zhang, and Y. Yao, "A deep learning framework about traffic flow forecasting for urban traffic emission monitoring system," *Frontiers Public Health*, vol. 9, Jan. 2022, Art. no. 804298.

[15] A. Nigam and S. Srivastava, "Hybrid deep learning models for traffic stream variables prediction during rainfall," *Multimodal Transp.*, vol. 2, no. 1, Mar. 2023, Art. no. 100052.

[16] X. Qi, G. Mei, J. Tu, N. Xi, and F. Piccialli, "A deep learning approach for long-term traffic flow prediction with multifactor fusion using spatiotemporal graph convolutional network," *IEEE Trans. Intell. Transp. Syst.*, pp. 1–14, 2022.

[17] H. Yang, L. Du, G. Zhang, and T. Ma, "A traffic flow dependency and dynamics based deep learning aided approach for network-wide traffic speed propagation prediction," *Transp. Res. B, Methodol.*, vol. 167, pp. 99–117, Jan. 2023.

[18] Bharti, P. Redhu, and K. Kumar, "Short-term traffic flow prediction based on optimized deep learning neural network: PSO-Bi-LSTM," *Phys. A, Stat. Mech. Appl.*, vol. 625, Sep. 2023, Art. no. 129001.

[19] C. Chen, B. Liu, S. Wan, P. Qiao, and Q. Pei, "An edge traffic flow detection scheme based on deep learning in an intelligent transportation system," *IEEE Trans. Intell. Transp. Syst.*, vol. 22, no. 3, pp. 1840–1852, Mar. 2021.

[20] K. Yu, L. Lin, M. Alazab, L. Tan, and B. Gu, "Deep learning-based traffic safety solution for a mixture of autonomous and manual vehicles in a 5G-enabled intelligent transportation system," *IEEE Trans. Intell. Transp. Syst.*, vol. 22, no. 7, pp. 4337–4347, Jul. 2021.

[21] C. Liu and L. Ke, "Cloud assisted Internet of Things intelligent transportation system and the traffic control system in the smart city," *J. Control Decis.*, vol. 10, no. 2, pp. 174–187, Apr. 2023.

[22] J. Chen, Y. Zhang, S. Teng, Y. Chen, H. Zhang, and F.-Y. Wang, "ACP-based energy-efficient schemes for sustainable intelligent transportation systems," *IEEE Trans. Intell. Vehicles*, pp. 1–4, 2023.

[23] M. H. Sulaiman and Z. Mustaffa, "An application of improved salp swarm algorithm for optimal power flow solution considering stochastic solar power generation," *e-Prime-Adv. Electr. Eng., Electron. Energy*, vol. 5, Sep. 2023, Art. no. 100195.

[24] F. Du, J. Zhang, N. Ji, G. Shi, and C. Zhang, "An effective hierarchical extreme learning machine based multimodal fusion framework," *Neurocomputing*, vol. 322, pp. 141–150, Dec. 2018.

[25] S. Aswath, V. R. S. Sundaram, and M. Mahdal, "An adaptive sleep apnea detection model using multi cascaded atrous-based deep learning schemes with hybrid artificial humming bird pity beetle algorithm," *IEEE Access*, vol. 11, pp. 113114–113133, 2023.

[26] M. Ragab, H. A. Abdushkour, L. Maghrabi, D. Alsalman, A. G. Fayoumi, and A. A.-M. Al-Ghamdi, "Improved artificial rabbits optimization with ensemble learning-based traffic flow monitoring on intelligent transportation system," *Sustainability*, vol. 15, no. 16, p. 12601, Aug. 2023.